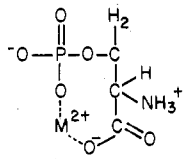

IV

that the phosphate moieties are not bound to the transition-metal ions for ML_2 and that the complexes are bis bidentate. Accordingly, the cumulative formation constants ($\beta = K_{ML}{}^{M}K_{ML_2}{}^{ML}$) of these complexes are quite similar to those where the ligand is alanine,[13] valine, or glycine.[2]

The analogous NMR experiment cannot be performed for ML with Cu(II), Ni(II), or Co(II) because this species is a minor component at ligand concentrations necessary to observe the phosphorus resonance. However, the equilibrium data show that ML complexes of SP are about 10 times more stable than those of alanine.[13] The most reasonable explanation for this difference is that the phosphate group is coordinated to the metal ion in ML and the ligand is tridentate.

For Co(II) and Ni(II) the structure of the ML_2 complex is less clear but appears to be analogous to that of Cu(II). For these metal ions, ML_3 species have appreciable formation constants and must be considered at high pH's and high ligand concentrations. It is clear that the phosphate groups do not bind the metal ions for ML_3, since broadening of the ^{31}P resonance is not observed for these species. Comparison of the change in ^{31}P line width to species concentration changes indicates that as in the Cu(II) case, the phosphate groups do not bind the metal ion in ML_2 for Co(II) or Ni(II); however, the fact that ML_2 does not predominate at any pH for these metals makes the determination more difficult.

It remains to offer an explanation for the difference in chelation by the amino acid phosphate esters in the ML and ML_2 complexes of transition-metal ions. This is most likely due to the high negative charge on the phosphate group. Evidently the charge repulsion of two phosphate groups bound to the same metal ion is so great as to prevent bis tridentate coordination. The large size of the chelate ring formed if phosphate coordinates in the ML_2 complex is unable to overcome the charge repulsion.

In the case of the alkaline earth metal ions the low stability of the ML complexes along with the relatively small increase in the acidity of the protonated amine group indicates that there is no significant binding by the nitrogen atom. Therefore, in these complexes, the amino acid phosphate esters bind Mg(II) and Ca(II) predominantly through their phosphate moieties.

Acknowledgment. The authors gratefully acknowledge support of this research under Grant AM 17015 from the National Institutes of Health.

Registry No. SP, 17885-08-4; TP, 27530-80-9; MSP, 66515-29-5; PEA, 1071-23-4; Cu, 7440-50-8; Ni, 7440-02-0; Zn, 7440-66-6; Co, 7440-48-4; Mn, 7439-96-5; Mg, 7439-95-4; Ca, 7440-70-2.

References and Notes

(1) (a) D. E. Metzler and E. E. Snell, *J. Biol. Chem.*, **198**, 353 (1952); (b) D. E. Metzler, J. B. Longenecker, and E. E. Snell, *J. Am. Chem. Soc.*, **76**, 639 (1954); (c) R. I. Gregermen and H. N. Christensen, *J. Biol. Chem.*, **220**, 765 (1956); (d) F. Binkley, *J. Am. Chem. Soc.*, **77**, 501 (1955); (e) F. Binkley and M. Boyd, *J. Biol. Chem.*, **217**, 67 (1955); (f) J. B. Longenecker and E. E. Snell, *J. Biol. Chem.*, **225**, 409 (1957); (g) T. H. Thomas, K. S. Dodgson, and N. Tudball, *Biochem. J.*, **110**, 687 (1968); (h) Y. Murakami, H. Kondo, and A. E. Martell, *J. Am. Chem. Soc.*, **95**, 7138 (1973).
(2) L. G. Sillen and A. E. Martell, *Chem. Soc., Spec. Publ.*, **No. 25**, (1971).
(3) *Biochem. Prep.*, **6**, 75, (1958).
(4) H. A. Flashka, "EDTA Titrations",, 2nd ed, Pergamon Press, Oxford, 1964.
(5) H. A. Harned and B. B. Owen, "The Physical Chemistry of Electrolytic Solutions", 3rd ed, Reinhold, New York, N.Y., 1958.
(6) I. G. Sayce, *Talanta*, **15**, 1397 (1968).
(7) A. Sabatani, A. Vacca, and P. Gans, *Talanta*, **21**, 53 (1974).
(8) P. Gans, A. Vacca, and A. Sabatani, *Inorg. Chim. Acta*, **18**, 237 (1976).
(9) E. V. Raju and H. B. Mathur, *J. Inorg. Nucl. Chem.*, **30**, 2181 (1968).
(10) M. M. Taqui Khan and A. E. Martell, *J. Am. Chem. Soc.*, **88**, 668 (1966).
(11) M. M. Taqui Khan and A. E. Martell, *J. Am. Chem. Soc.*, **84**, 3037 (1962).
(12) G. Schwarzenbach and G. Anderegg, *Helv. Chim. Acta*, **40**, 1229 (1957).
(13) V. S. Sharma and H. B. Mathur, *Indian J. Chem.*, **3**, 476 1965.

Contribution from the Chemistry Division,
Oak Ridge National Laboratory, Oak Ridge, Tennessee 37830

Telluride Ion Chemistry in Molten Salts

L. M. TOTH* and B. F. HITCH

Received February 14, 1978

The Te^- ion has been shown to be the dominant telluride ion present in molten LiCl–KCl (59–41 mol %) and LiF–BeF_2 (66–34 mol %). It is characterized by an intense band at 497 and 478 nm in the respective solvents, ϵ 3370 L mol^{-1} cm^{-1}, and has a solubility limit of 8×10^{-3} mol % at 550 °C in the chloride melt. Higher tellurides such as Te_3^- are also suggested in the chloride melts by the shift of the 497-nm band and the appearance of a second band at 650 nm. Prerequisites to reliable telluride ion control in molten salt solutions have been shown to be (1) the maintenance of Te_2 vapor in equilibrium with the melts and (2) the prevention of melt contact with oxidizing container materials such as silica.

Introduction

In contrast to the detailed studies[1] reported for tellurium cations, Te_m^{n+}, in high-temperature molten salts, little information is available for the corresponding tellurides in these media. Gruen et al.[2] have reported on the behavior of Li_2Te, Cs_2Te, and Te in molten chlorides at temperatures of 400–1000 °C and have suggested that the soluble telluride species giving rise to a weak band at 471 nm (ϵ 30 L mol^{-1} cm^{-1}) was the Te^{2-} ion. They further suggested that through solvation with the alkali metal ions, the net formal charge on the tellurium was reduced to 1.1– and 1.2– for the lithium and cesium telluride solutions, respectively. More recently, Bamberger et al.[3] examined various telluride species in molten LiF–BeF_2 (66–34 mol %) from 525 to 650 °C and observed a similar band at 478 nm. By prereduction of the melt with silicon to remove oxidizing impurities, they demonstrated that Te^{2-} either had no absorbance in the 200–2000-nm region or, if it did, was too insoluble in the molten fluoride solution to be detected. They therefore suggested that the species giving rise to the band at 478 nm was of higher oxidation state than Te^{2-} and was, most likely, Te_3^-.

Both of these groups used silica cells to contain the telluride solutions and they both noted chemical instability of the solutions due to a reaction with the container accompanied by vapor-phase transport of tellurium metal to colder regions of the cell. As a result of these experimental difficulties, the

0020-1669/78/1317-2207$01.00/0

exact nature of the Te_m^{n-} ion in these molten salts and its chemical behavior was never clearly established and still remains a subject of some debate.

To adequately control the redox chemistry of tellurium in solution, the impurity reactions and tellurium vapor transport must be eliminated. These two provisions were incorporated in the present study and have led to the identification of the dominant telluride ion in solutions of selected molten chlorides and fluorides. We were not able to extensively study telluride ion chemistry in molten salts, but the identification of the basic tellluride ion in solution, which is of considerable significance to molten salt reactor technology,[4] and circumstances which enable its control are now known.

Experimental Section

Reagents. The lithium tellurides, Li_2Te and $LiTe_3$, were obtained from Valentine.[5] Chemical analysis showed the following. Anal. Calcd for Li_2Te: Li, 9.9; Te, 90.1. Found: Li, 9.5 ± 0.1; Te, 89.9 ± 0.5; O, 740 ppm. Anal. Calcd for $LiTe_3$: Li, 1.8; Te, 98.9. Found: Li, 1.7 ± 0.1; Te, 98.4 ± 0.5; O, 275 ppm. The tellurium metal was taken from 99.999+% pure material obtained from Alpha Ventron Products.

The molten salts were purified by standard purification procedures; i.e., by sparging with the anhydrous halide gas, HF or HCl, followed by helium that had been dried and deoxygenated by passage through a titanium sponge trap held at 700 °C. In some instances the melts were contacted either with zirconium metal or with hydrogen to ensure that no oxidizing impurities were present.

Procedure. Silica Containment. The initial work on tellurides in the LiCl–KCl eutectic was performed in silica cells similar to those used in the two previous investigations. The cell design and procedure were standard for molten salt work at this laboratory.[6] The cell consisted of a 1-cm path length cuvette fitted to a 17-mm o.d. silica tube to which was attached a 24/40 standard taper joint. The cell was cleaned and then degassed under vacuum at approximately 800 °C and transferred to a helium-filled inert-atmosphere (less than 1 ppm H_2O and O_2) glovebox for all reagent handling operations. The sample components were loaded and the capped cell was taken to a vacuum manifold for sealing under a vacuum or $^1/_3$ atm of dry helium, as the circumstances dictated. The total volume of the cell was approximately 25 cm^3 and contained 3.5 cm^3 of molten salt.

Diamond-Windowed Graphite Cell Containment. Because all molten salt solutions containing tellurides corroded the silica cells severely, a diamond-windowed graphite cell[7] was used to contain the melts. The graphite cell was loaded in a fashion similar to that which was followed for the silica cell and was fitted with a graphite plug to prevent the molten salt from spilling out during mixing. The plug had a small breather hole which allowed the Te_2 vapor inside the cell to equilibrate with the entire gas space of the silica envelope. The cell was sealed in a silica tube which prevented escape of Te_2 vapor and exposure of the graphite cell and contents to the laboratory atmosphere. In all other respects the procedure was the same as that used for the silica cells.

The silica-enclosed graphite cell was allowed to equilibrate for a half day or more at 450–700 °C while being rocked in a horizontal position. After equilibration, the cell was transferred to a preheated furnace[8] which, for these experiments, had been placed on its side. To prevent mass transport of tellurium from the melt, a temperature gradient of approximately 10 °C was established in the furnace so that the melt was cooler than the gas space above it. Since the cell had been designed to hold a small liquid volume (<0.5 cm^3), surface tension held the solution in the window zone even though the cell was on its side. Gentle rocking, on the other hand, sufficed to dislodge the liquid and provide mixing when necessary. With the graphite cell in the lowest position (cf. Figure 1), the absorption spectrum of the solution could be measured, and, with the cell in the highest position, the spectrum of the vapor could be obtained through the 1.6-cm path length of the silica tube. A correction was made for the small amount of vapor between the diamond windows and the silica tube whenever necessary.

Reagents could be added during the course of a run by cooling the sample to 25 °C, transferring it to the inert-atmosphere glovebox, breaking open the silica envelope surrounding the graphite cell, and placing appropriate amounts of tellurium and/or lithium tellurides inside the graphite cell. The cell would then be sealed in a new silica tube and reheated for further measurements. Even though some of the tellurium metal was lost in discarding the broken silica envelope to which condensed metal had adhered, the loss frequently amounted to only a few percent of the inventory in the cell and did not severely alter the material balance necessary for determining the molar extinction coefficient of the soluble telluride species. Otherwise the material balance was unimportant because absorption spectra measurements were used to determine Te_2 vapor pressures at equilibrium in situ. No loss of lithium tellurides occurred during this procedure because they remained inside the graphite cell.

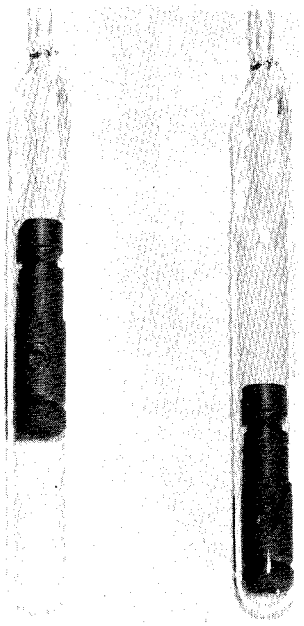

Figure 1. Diamond-windowed graphite cell used to contain molten salt solutions of lithium tellurides. Te_2 vapor spectra and melt spectra were measured with cell in upper and lower positions, respectively.

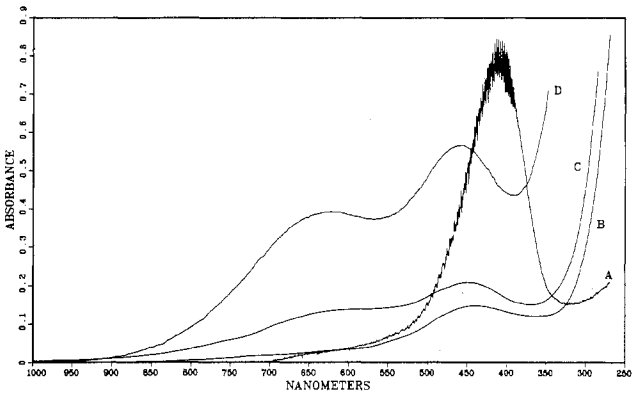

Figure 2. Typical spectra of Te_2 in a 1-cm path length cell: (A) vapor at 706 °C, (B) LiCl solution at 781 °C, (C) LiCl–KCl eutectic solution at 747 °C, (D) CsCl solution at 665 °C (×0.25).

Spectral Measurements. Absorption spectra of the melt and the vapor in equilibrium with it were separately scanned using a Cary 14H recording spectrophotometer equipped with a Datex digital output accessory. A 0.0–0.1 absorbance slide wire was used for the vapor measurements whenever necessary. Distortion of the spectrometer light due to passage through the curved silica tubing was found to be negligible as long as the tube was properly aligned.

Results and Discussion

Te_2 Spectra in Molten Salts. Absorption spectra of Te_2 in the vapor and in molten LiCl, LiCl–KCl (eutectic), and CsCl were measured to correct telluride solute spectra for soluble Te_2. The Te_2 vapor spectrum has already been reported[9,10] and is shown in Figure 2A for comparison with the melt spectra. The Te_2 spectrum is characterized by a broad band at 410 nm with vibronic structure for the species in the vapor

(ϵ 3600 L mol^{-1} cm^{-1}).[10] A similar band appears at 450 nm for Te_2 in molten LiCl, Figure 2B, but the spectrum does not show the vibronic structure. In CsCl, Figure 2D, a band at 450 nm occurs along with a second band at 650 nm. These two bands do not vary in an internally consistent fashion (as was expected for a single species obeying Beer's law) since, at low Te_2 vapor pressures, the 450-nm band is less intense than the 650-nm band. The behavior of the 650-nm band therefore suggests that it is due to a second tellurium species which is formed by a redox reaction with an impurity in the melt. A much smaller band at 650 nm is also observed in the LiCl–KCl eutectic melt and is likewise attributed to an impurity reaction. (Note that the intensity of the Te_2 spectrum in CsCl, for an equivalent weight of Te metal added (0.18 g in 3.5 cm^3 of melt) is reduced by a factor of 0.25 in the figure.)

Although time did not permit an extensive effort in solvent purification that would eliminate the 650-nm band in CsCl or LiCl–KCl, the Te_2 melt spectra demonstrate that the 650-nm band is not typical of Te_2 and that, because of its behavior in relation to the one at 450 nm, the band is probably due to an impurity reaction. The spectrum of Te_2 in these molten salts is therefore best represented by that of Figure 2B, and the Te_2 solubility in the LiCl–KCl solvent at 550 °C has a Henry's law coefficient of $K = 8 \times 10^8$ mm. With such a solubility dependence on pressure, there was no need to make any corrections for Te_2 melt absorbance in the telluride experiments requiring less than a hundreth of that used to produce the band in Figure 2C.

Melt Spectra. As stated earlier, the principal goal of this work was to identify the telluride ion species present in selected molten chlorides and fluorides. Since the earlier studies had been performed in silica cells, some of our initial measurements were also made in silica to provide both a means of assessing the previous results and a basis for comparison of results obtained with the diamond cell.

Tellurium alone in the molten LiCl–KCl eutectic gave no sign of reaction at temperatures up to 800 °C. The addition of Li_2Te, however, caused a corrosive attack on the silica with the accompanying oxidation of the telluride. For example, when 2 mg of Li_2Te was sealed in a cell with 3.5 g of the LiCl–KCl eutectic and the system was agitated at 500 °C, color appeared in the melt almost immediately and grew to the deep burgundy color reported by Gruen et al.[2] A spectrum of the solution revealed a band at 497 nm which, after 1 week at 550 °C in the 1-cm path length cell, reached an intensity of approximately six absorbance units. Etching of the silica cell was obvious during the second day of exposure and, after a week, the etch had penetrated almost halfway through the 1-mm silica wall. Ultimately, the characteristic yellow Te_2 vapor appeared over the melt adding to the evidence of Li_2Te oxidation. We therefore suggest an oxidative reaction occurs between the telluride and the silica and thereby prevents the stabilized control of the tellurium redox chemistry in silica systems.

In contrast to the behavior in silica cells, chloride and fluoride melts containing Li_2Te in diamond-windowed graphite cells produced no bands[11] in the 400–2500-nm region, even after a week's duration at 500 °C. These comparative studies demonstrated that silica cells were only suitable for Te_2 solutions and that the diamond-windowed graphite cell was essential for reliable control of telluride ions in solution.

With the necessity of avoiding the use of silica cells thus established, the general description of our work on tellurides in molten salts can best be presented in two parts: the first is concerned with the occurrence and identification of the simplest telluride ion, common to all solvents investigated; the second deals with the varying behavior observed in the solvents when the solubility limit of the sample species is reached and/or the oxidation potential of the system is raised above that of the simple species.

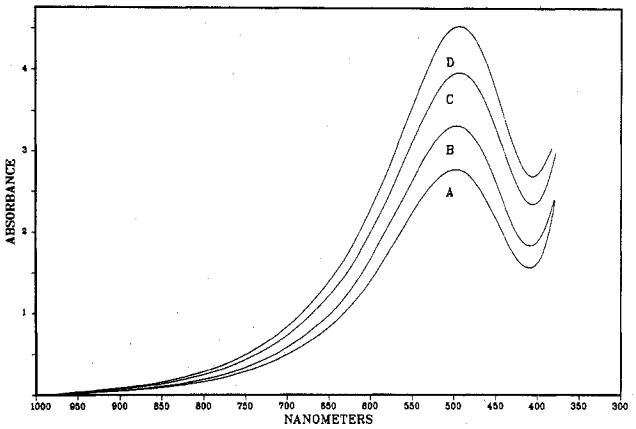

Figure 3. Effect of titrating Li_2Te with Te_2 in the LiCl–KCl eutectic at 550 °C. Four separate additions produce successive increases in the 497-nm band. These data are plotted in Figure 4 along with the measured Te_2 absorbance.

Identification of Te^- Ion. Li_2Te gave no color in the molten salt solutions, but the addition of Te_2 to a system already containing Li_2Te produced a band at 497 nm with an intensity that was proportional to the amount added. Spectra representing the effect of such a "titration" are shown in Figure 3 for several additions of Te_2 as described in the Experimental Section. Expecially significant is the unchanged position of the 497-nm band as its intensity increases to approximately five absorbance units. When the top of the cell was cooled slightly so that tellurium metal deposited on the silica envelope away from the melt, the intensity of the 497-nm band decreased accordingly. Reversal of the temperature gradient caused the original intensity of the band to return, thus demonstrating the concentration dependence of the soluble species on the Te_2 overpressure.

A Beer's law test was, for all practical purposes, impossible to perform on the species in solution because its concentration depended directly on the Te_2 pressure. Nevertheless, the unaltered band profile and position throughout the titration justifies the assumption that a single species was produced by the reaction

$$n\mathrm{Li_2Te(c)} + m\mathrm{Te_2(g)} \rightleftarrows 2\mathrm{Te}_{(n/2)+m}^{n-} + 2n\mathrm{Li^+} \quad (1)$$

where the dissolved (d) telluride species on the right is responsible for the 497-nm band.

The identity of this soluble telluride was determined by adding a substantial excess of Li_2Te to ensure saturation of the melt[12] and then titrating with Te_2 while measuring both the Te_2 vapor spectrum and 497-nm band in the melt after each addition. Neglecting the change of the Li^+ concentration in the LiCl–KCl solution as a result of eq 1, a plot of the log (Te_2 vapor absorbance) vs. log (497-nm band absorbance) yields the results in Figure 4 where the slope of the line is equal to half the stoichiometric factor m of eq 1. Typical slopes are shown by lines A, B, and C for $m = {}^5/_2$, ${}^3/_2$, and ${}^1/_2$ (i.e., for the Te_3^-, Te_2^-, and Te^- soluble species when $n = 1$), respectively, from which a value of $m = {}^1/_2$ is readily apparent. Therefore when $m = {}^1/_2$, meaningful solutions to the above equation occur for $n = 1, 3, 5, \ldots$, etc., and in the simplest case, $n = 1$, the species would be the Te^- ion.

For the Te_2^{2-} ion to occur, values of $m = 1$ and $n = 2$ are required. Although the scatter of the data in the lower part of the figure could be viewed as significant (with slope $\approx {}^1/_2$) and consequently indicative of Te_2^{2-} occurring at lower Te_2 pressures, the constant position and profile of the 497-nm band throughout the titration point most clearly to a single-species interpretation. Furthermore, the solubility of the $Te_{(n/2)+m}^{n-}$

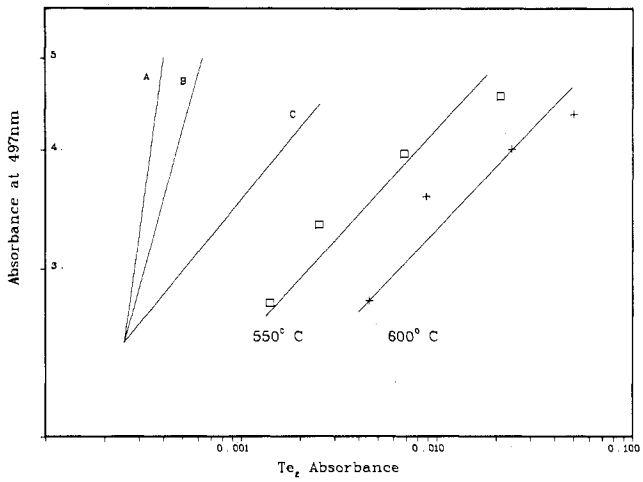

Figure 4. Plot of $Te_{(n/2)+m}^{m-}$ species absorbance at 497 nm as a function of Te_2 vapor absorbance at 550 and 600 °C. Typical slopes shown in A, B, and C for stoichiometric factor, m of eq 1, equal to $^5/_2$, $^3/_2$, and $^1/_2$, respectively.

species in the fluoride melt supports the monoatomic, Te^-, identification and dismisses the occurrence of polyatomic species that would result if $m = {}^1/_2$ and $n = 3, 5, \ldots$, etc. (cf. discussion under Other Telluride Species).

On the basis of these considerations, we conclude that the dominant telluride species in the chloride and fluoride melts studied here is the Te^- ion and eq 1 becomes

$$Li_2Te(c) + {}^1/_2Te_2(g) \rightleftarrows 2Te^-(d) + 2Li^+(d) \quad (2)$$

From the change in Te^- absorbance with Te_2 pressure, the molar absorptivity of the Te^- ion is estimated to be 3370 L mol^{-1} cm^{-1}. The solubility limit of Te^- at 550 °C as suggested by the maximum five absorbance measured in the 0.635-cm cell is found to be 8×10^{-3} mol % and the equilibrium quotients for the formation of LiTe(d) at 550 and 600 °C are 1.42×10^{-6} and 8.7×10^{-7} $atm^{-1/2}$, respectivity. If the standard state of the system is chosen so that the activity coefficient of LiTe is unity when present in small amounts in the LiCl–KCl eutectic melt, the free energies of reaction using this standard state are 21.9 and 24.1 kcal for 550 and 600 °C, respectively.

The identification of the Te^- ion in melts is consistent with the observations of Manning,[13] who perceived a one-electron process to occur from polarization experiments at a tellurium electrode. This conclusion is also consistent with the results of Bamberger et al.,[3] but, because of the limited scope of their study, they chose to interpret the soluble species in fluoride melts as Te_3^-. Although Li_2Te and $LiTe_3$ are the only two telluride phases that have been found in Li–Te phase studies, the solvation effects of the molten salts most probably stabilize the Te^- ion sufficiently, causing it to be the dominant species in solution.

Other Telluride Species. For oxidation potentials in excess of that required to produce Te^- or for Te_2 additions in excess of that required to produce a saturated solution of Te^- in the molten salt when an Li_2Te phase is present, the behavior of tellurides in chloride and fluoride melts diverges. In the LiCl–KCl eutectic, the 497-nm band shifts progressively to lower wavelengths and a new band at 650 nm appears. The two curves in Figure 5 exemplify the difference in the spectrum of Te^-, curve A, and that of the telluride solution at higher oxidation potentials, i.e., Te_2 additions over those required to produce Te^-. The spectrum in Figure 5B is also observed if $LiTe_3$ is dissolved in a pure LiCl–KCl eutectic solvent mixture. Distillation of Te_2 from the melt produces a reversible shift of the 475-nm band back to the 497-nm position with the simultantous disappearance of the 650-nm band. In contrast

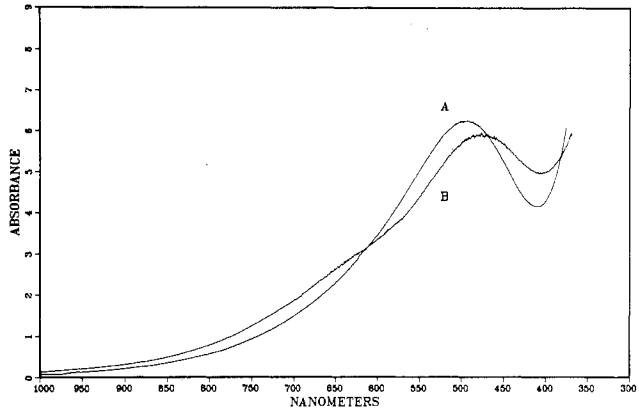

Figure 5. Effect of exceeding oxidation potential of Te^- ion in LiCl–KCl eutectic solvent to produce higher telluride species as seen by shift of the 497-nm band, curve A, to 450 nm and appearance of a 650-nm shoulder, curve B.

to the behavior in the LiCl–KCl solvent, no shift in the 478-nm band is observed in the molten fluoride solution and no 650-nm band is seen. These phenomena in the chloride melt are interpreted as arising from higher tellurides (such as Te_3^-) that are formed when the oxidation potential is increased. The higher tellurides probably are not observed in the molten fluorides simply because of differences in solubility of the tellurides in the chloride and fluoride solvents. Reflecting back on the nature of the Te^- ion in solution, these same arguments support the conviction that Te^- occurs as a simple monatomic ion and not a $(Te^-)_n$ aggregate.

In conclusion, the Te^- ion has been shown to be the dominant telluride species present in molten chlorides and fluorides studied to date. This is the same species seen by the previous authors, but incorrectly identified as either Te^{2-} or Te_3^-. The absorption coefficient of the 497-nm band is quite large—in contrast to that estimated by Gruen[2]—indicating that the band is due to an allowed 5p–5d or 5p–6s electronic transition. It is interesting to note that Gruen suggested a formal charge of approximately 1– on the alkali-metal solvated telluride ion by comparing the atomic transition energies for a series of elements in the region of the periodic table around tellurium. The only difference with our data is that the 1– represents the formal charge on the ion regardless of solvation. Finally, the occurrence of higher tellurides in chloride melts is strongly indicated by the blue shift of the 497-nm band and the appearance of the 650-nm band.

Acknowledgment. Research was sponsored by the Division of Basic Energy Sciences, Department of Energy, under contract with Union Carbide Corp. The authors gratefully acknowledge the many helpful comments offered by A. D. Kelmers and L. M. Ferris during the course of this work.

References and Notes

(1) See, for example, N. J. Bjerrum, *Inorg. Chem.*, **11**, 2648 (1972); **10**, 2578 (1971); **9**, 1965 (1970).
(2) D. M. Gruen, R. L. McBeth, M. S. Foster, and C. E. Crouthamel, *J. Phys. Chem.*, **70**, 472 (1966).
(3) C. E. Bamberger, J. P. Young, and R. G. Ross, *J. Inorg. Nucl. Chem.*, **36**, 1158 (1974).
(4) L. E. McNeese and M. W. Rosenthal, *Nucl. News (Hinsdale, Ill.)*, **17**, 52 (1974).
(5) For details of preparation, see D. Y. Valentine, O. B. Cavin, and H. L. Yakel, *Acta Crystallogr., Sect. B*, **33**, 1389 (1977).
(6) See, for example G. P. Smith and C. R. Boston, *J. Chem. Phys.*, **43**, 4051 (1965).
(7) L. M. Toth, J. P. Young, and G. P. Smith, *Anal. Chem.*, **41**, 463 (1969).
(8) L. M. Toth and L. O. Gilpatrick, *J. Phys. Chem.*, **77**, 2799 (1973).
(9) R. F. Brebrick and A. J. Strauss, *J. Chem. Phys.*, **40**, 3230 (1964).
(10) B. F. Hitch, L. M. Toth, and J. Brynestad, *J. Inorg. Nucl. Chem.*, **40**, 31 (1978).
(11) Incomplete removal of residual hydrogen halide sparge gas or some excess Te in the Li_2Te phase can cause traces of color to appear when Li_2Te is added. The great intensity of the 497-nm band (see later part of

discussion) makes elimination of all color difficult to achieve when large Li_2Te additions are made. Active metal prereduction of molten salt solvents has been found useful in controlling the oxidizing impurities.

(12) It has been shown that the solubility of Li_2Te in molten fluorides is less than 10^{-5} mole fraction (see L. E. McNeese, "Molten Salt Reactor Program Semiannual Progress Report for Period Ending Feb. 29, 1976", ORNL-5132, Oak Ridge National Laboratory, Oak Ridge, Tenn., p 24). Our addition, equivalent to 10^{-3} mole fraction, caused the appearance of a separate Li_2Te phase.

(13) D. L. Manning and G. Mamantov in "Characterization of Solutes in Nonaqueous Solvents", G. Mamantov, Ed., Plenum Press, New York, N.Y., 1978.

Contribution from the Department of Chemistry,
The University of North Carolina, Chapel Hill, North Carolina 27514

Synthesis and Properties of the Chloro-Bridged Dimer $[(bpy)_2RuCl]_2^{2+}$ and Its Transient 3+ Mixed-Valence Ion

EUGENE C. JOHNSON, B. P. SULLIVAN, DENNIS J. SALMON, S. AJAO ADEYEMI, and THOMAS J. MEYER*

Received November 9, 1977

A new di-μ-chloro dimer, $[(bpy)_2RuCl]_2^{2+}$, has been synthesized. The Ru(II)–Ru(II) form of the dimer has been shown to undergo symmetrical bridge cleavage reactions in the presence of added ligands such as CH_3CN and is a convenient precursor to complexes of the type $(bpy)_2RuL(Cl)^+$. Cyclic voltammetry studies show that the dimer undergoes two reversible one-electron oxidations corresponding to stepwise oxidations at the two metal sites. Controlled-potential electrolysis just past the first oxidation wave results in the unsymmetrical cleavage of the transient mixed-valence dimer $[(bpy)_2RuCl]_2^{3+}$ to give $Ru(bpy)_2Cl_2^+$ and monomeric Ru(II) complexes. A simple molecular orbital rationale of this behavior is given in terms of weak interactions between the Ru sites in the 2+ dimer and localized Ru(II) and Ru(III) sites in the transient, mixed-valence dimer.

We describe here the preparation and properties of the dimeric ion $[(bpy)_2RuCl]_2^{2+}$ (bpy is 2,2′-bipyridine). Our interest in the ion has two origins. Halide-bridged dimers and higher oligomers have frequently been used successfully as synthetic intermediates based on, what are often, facile bridge cleavage reactions:

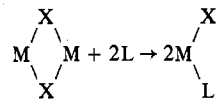

$$M\begin{smallmatrix}X\\X\end{smallmatrix}M + 2L \rightarrow 2M\begin{smallmatrix}X\\L\end{smallmatrix}$$

We and others have shown that bpy complexes of ruthenium can be of great value in the study of such diverse phenomena as excited-state redox and sensitization processes,[1] mixed-valence chemistry,[1c,2] electron-transfer processes,[3,4] and reactions of coordinated ligands.[5] In many of these studies controlled chemical syntheses are an essential feature, and $[(bpy)_2RuCl]_2^{2+}$ is a potentially useful source of the $(bpy)_2Ru^{II}Cl$ moiety.

A continuing problem in mixed-valence chemistry is to understand how details of molecular structure influence the extent and nature of electronic interactions between metal sites. One-electron oxidation of $[(bpy)_2RuCl]_2^{2+}$ would give a 3+ mixed-valence ion. From known chemical examples there are several possibilities for the orbital nature of the Ru–Ru interaction and for the effect of the Ru–Ru interaction on the properties of the ion. In the dimer $(bpy)_2ClRu^{II}(pyr)Ru^{III}Cl(bpy)_2^{3+}$ there are discrete Ru(II) and Ru(III) sites, and delocalization between them is slight.[6] Electronic orbital overlap between the Ru(II) and Ru(III) sites does occur promoted by $d\pi(Ru(II))$–π^*(pyrazine) mixing, but overlap is small and there are localized redox sites on the vibrational time scale. With enhanced overlap the sites can become vibrationally equivalent and the system delocalized. In oxo-bridged ions like $(bpy)_2ClRuORuCl(bpy)_2^{2+}$, it has been concluded that strong $d\pi(Ru)$–$p(O)$–$d\pi(Ru)$ mixing leads to delocalized molecular orbitals and that gain or loss of electrons to give the 1+ and 3+ mixed-valence ions occurs from these delocalized levels.[7,8] Extensive $d\pi(Ru)$–$p(Cl)$–$d\pi(Ru)$ mixing could lead to the same type of case in $(bpy)_2RuCl_2Ru(bpy)_2^{3+}$. Oxidation of $[(bpy)_2RuCl]_2^{2+}$ could also occur by loss of an electron from an orbital largely antibonding Ru–Ru in character to give a partial metal–metal bond. This is apparently the situation which does occur both in $(PBu^n_3)_2ClRuCl_3RuCl(PBu^n_3)_2$[9] and in the electronically analogous iron dimer $(\pi\text{-}C_5H_5)(CO)Fe(SMe)_2Fe(CO)(\pi\text{-}C_5H_5)^+$.[10] There is a further interesting example in the tri-μ-chloro-bridged "Ru blue" ions like $[(NH_3)_3RuCl_3Ru(NH_3)_3]^{2+}$ where the Ru–Ru interaction is striking in its effect upon the electronic spectra of the ions,[11] but the orbital nature of the Ru–Ru interaction in unclear in the absence of supporting structural data.

There are many examples of chloro-bridged ruthenium compounds including the cluster $Ru_5Cl_{12}^{2-}$,[12] dimers involving triply bridging chlorides as in the dimers above or in $(PPhEt_2)_3RuCl_3Ru(PPhEt_2)_3^+$,[13] and dimers involving doubly bridging chlorides as in $[(CO)_3RuCl_2]_2$,[14] $[(\pi\text{-}C_6H_6)RuCl_2]_2$,[15] $[(bpy)(PPh_3)_2RuCl]_2^{2+}$,[16] $[(CHT)RuCl_2]_2$[17] (CHT = cycloheptatriene), or $(CS_2)(PPh_3)_2RuCl_2$.[18] There are also reports of a dimer having a single chloride bridge, $[(NH_3)_3(H_2O)RuCl_2]_2^+$,[19] and of three chloride-bridged polymers, $[(norb)RuCl_2]_x$[20] (norb = norbornadiene), $[(CO)_2RuCl_2]_x$,[17] and $[(COD)RuCl_2]_x$ (COD = cycloocta-1,5-diene).[17,21]

Experimental Section

Physical Measurements. Infrared spectra were recorded on a Perkin-Elmer 421 spectrophotometer in potassium bromide pellets at room temperature. Ultraviolet–visible spectra were recorded on Cary Model 14, Cary Model 17, Unicam Model SP800B, or Bausch and Lomb Spectronic 210 UV spectrophotometers in 1- and 10-mm cells at room temperature. ESCA measurements were obtained on a du Pont Instruments 650 electron spectrometer equipped with a du Pont Instruments multichannel analyzer. Samples were prepared by grinding the solid complex into the surface of a gold sample probe using a clean glass rod. Electrochemical studies were conducted vs. the saturated sodium chloride calomel electrodes (SSCE) using 0.1 M tetrabutylammonium hexafluorophosphate (TBAH) as the supporting electrolyte. The measurements were recorded using a Princeton Applied Research Model 173 potentiostat/galvanostat with a Model 176 electrometer probe and standard three-electrode operational amplifier circuitry. A Princeton Applied Research Model 175 universal programmer was employed as a signal generator for voltammetric and chronoamperometric measurements.

Materials. Acetonitrile (MCB, Spectrograde) was used without further purification for all spectroscopic studies. Water was deionized and redistilled from alkaline $KMnO_4$ using an all-glass apparatus. All other solvents (reagent grade) were purchased commercially and

0020-1669/78/1317-2211$01.00/0